QUARTERLY JOURNAL
OF THE
ROYAL METEOROLOGICAL SOCIETY

Vol. 130 OCTOBER 2004 Part C (EUROCS) No. 604

Q. J. R. Meteorol. Soc. (2004), **130**, pp. 3055–3079 doi: 10.1256/qj.03.130

Sensitivity of moist convection to environmental humidity

By S. H. DERBYSHIRE[1]*, I. BEAU[2], P. BECHTOLD[3,4], J.-Y. GRANDPEIX[5], J.-M. PIRIOU[6], J.-L. REDELSPERGER[6] and P. M. M. SOARES[7,8]

[1]*Met Office, Exeter, UK*
[2]*Météo-France/ENM, Toulouse, France*
[3]*Observatoire Midi-Pyrénées, Toulouse, France*
[4]*European Centre for Medium-Range Weather Forecasts, Reading, UK*
[5]*Laboratoire de Météorologie Dynamique, Paris, France*
[6]*Météo-France/CNRM, Toulouse, France*
[7]*Instituto Superior de Engenharia de Lisboa, Portugal*
[8]*Centro de Geofisica da Universidade de Lisboa, Portugal*

(Received 24 July 2003; revised 27 May 2004)

SUMMARY

As part of the EUROCS (EUROpean Cloud Systems study) project, cloud-resolving model (CRM) simulations and parallel single-column model (SCM) tests of the sensitivity of moist atmospheric convection to mid-tropospheric humidity are presented. This sensitivity is broadly supported by observations and some previous model studies, but is still poorly quantified. Mixing between clouds and environment is a key mechanism, central to many of the fundamental differences between convection schemes.

Here, we define an idealized quasi-steady 'testbed', in which the large-scale environment is assumed to adjust the local mean profiles on a timescale of one hour. We then test sensitivity to the target profiles at heights above 2 km.

Two independent CRMs agree reasonably well in their response to the different background profiles and both show strong deep precipitating convection in the more moist cases, but only shallow convection in the driest case. The CRM results also appear to be numerically robust. All the SCMs, most of which are one-dimensional versions of global climate models (GCMs), show sensitivity to humidity but differ in various ways from the CRMs. Some of the SCMs are improved in the light of these comparisons, with GCM improvements documented elsewhere.

KEYWORDS: Cumulus convection Humidity sensitivity Model intercomparison

1. INTRODUCTION

This study seeks to evaluate the sensitivity of cumulus convection to humidity in the free troposphere, using cloud-resolving models (CRMs) and comparisons with single-column models (SCMs), in order to help improve the performance of convection representation in global climate models (GCMs). The work forms part of the EUROCS (EUROpean Cloud Systems study) project.

Moist convection is subject to many influences and interactions. Classical convection theory, using the adiabatic parcel model, emphasizes the temperature and humidity of the boundary layer and the temperature of the free tropospheric environment within which convective clouds may develop. In reality other processes play significant roles,

* Corresponding author: Met Office, FitzRoy Road, Exeter EX1 3PB, UK.
e-mail: steve.derbyshire@metoffice.gov.uk

including forms of triggering or inhibition, the retention or precipitation of condensate, freezing and melting, downdraughts and other cloud-system circulations and the mixing between clouds and environment.

As noted by Raymond and Zeng (2000), simple arguments suggest a relationship between atmospheric humidity and the 'propensity for precipitation'. However, the relationship is not adiabatic but depends on the rate of mixing. Assuming an effective condensation process which rapidly removes supersaturation with respect to water, the temperature, T, of a saturated parcel at any given height, z, is essentially a function of the moist-static-energy temperature, $T_h = T + (gz + Lq_\mathrm{v})/c_p$ (in standard notation). For example, if 'plume' and 'environmental' air were to mix in a 1:1 ratio, then each 1 g kg^{-1} subsaturation of the 'environment' would detract $\sim$1.25 K from the h_T of the dilute mixture, and hence significantly reduce its buoyancy. But in adiabatic parcel theory, environmental humidity plays no role in convective stability, beyond a small direct 'virtual temperature' contribution, except at the source of the parcel itself (usually assumed to be the boundary layer). Hence quantification of humidity impacts touches on fundamental issues in representing moist convection.

There are other reasons to suspect that humidity impacts via mixing may be important for large-scale modelling. Riehl (1954, p.380) concluded from an analysis of trade-wind regions that 'the entrainment responsible for limiting the vertical growth of cumuli . . . may have far-reaching consequences for the general circulation'. Johnson (1997) reviewed observations from the tropical TOGA–COARE* campaign, showing strong associations between humidity in the free atmosphere and the occurrence of strong organized convection (see also Zhang *et al.* (2003) and references therein). Raymond (2000) speculated that tropical rainfall is primarily controlled by the mean saturation deficit of the troposphere but stressed the need for further information of how convective properties depend on their environment to resolve the long-standing questions about convective controls. Grabowski (2003) found that features resembling an idealized Madden–Julian oscillation in aquaplanet simulations using his CRCP 'superparametrization' seem to depend on the humidity–convection link, and can be suppressed by artificially suppressing this link. This suggests that humidity impacts are dynamically significant, through relationships with vertical motion.

CRM studies can now provide more detailed evidence. Redelsperger *et al.* (2002) simulated a TOGA–COARE case based on an observed dry intrusion event, and found strong positive associations between mean humidity between 2–6 km and convective cloud-top heights. These associations were stronger in this case study than any associations with CAPE†. Their results support, at least qualitatively, some significant predictions of the entraining plume model of moist convection. In an idealized CRM study, Tompkins (2001a) showed that sensitivity to free-tropospheric humidity plays an important role in the organization of tropical convection. He showed this by artificially perturbing the free-tropospheric humidity, and gave further observational and theoretical support. Tompkins (2001b) further analysed the role of downdraughts and cold pools in organizing convection.

Yet, despite broad observational and CRM support for impacts of mid-tropospheric humidity on convection, the specific implications for parametrization remain poorly understood. Updraught entrainment is not the only mechanism, and its interpretation is complicated by the complexity of mixing in realistic convective cloud fields (e.g. Blyth *et al.* 1988). Attempts to estimate the variability in such mixing (as it affects

* Tropical Ocean Global Atmosphere–Coupled Ocean/Atmosphere Response Experiment.

† Convective Available Potential Energy.

convective transport properties) are made by several well-known schemes, including those of Arakawa and Schubert (1974), Kain and Fritsch (1990), Emanuel (1991), and Donner (1993). More recently some steps have been taken towards the representation of a convective cloud field using ideas from turbulence theory (Grant and Brown 1999; Khairoutdinov and Randall 2002).

As with other difficult issues in convection parametrization, it is now natural to look to CRMs and intercomparisons as a systematic avenue for progress. For example, Ridout (2002) ran quasi-cloud-resolving-model forecasts of a case study within a nested framework, identified humidity impacts and compared with two parametrization schemes. The present study complements that work, using a more idealized case, much higher CRM resolution and a wider intercomparison of schemes geared to testing quantitatively their sensitivity to humidity.

The CRMs represented here have been tested against a range of observational case studies (e.g. Xu *et al.* 2002) and such comparisons form an important part of the EUROCS project. However we can also run more idealized CRM cases to test individual parameter sensitivities that are critical for parametrization. The present CRMs (see section 2 for more details) are well adapted to the evaluation of mixing and its impacts, having been designed and tested in problems of boundary-layer turbulence as well as convective cloud systems. The SCMs represented here include a variety of statistical approaches to convective mixing.

2. Method

The overall methodology of this study is to intercompare CRM and SCM sensitivities to mid-tropospheric humidity, using a testbed relevant to the performance of convection parametrization in GCMs. For such a comparison to help improve the SCMs we wish (1) to have greater consistency in the CRMs than in the current SCMs and (2) to devise tests that are neither too hard nor too easy for the SCMs.

We concentrated in this part of the EUROCS project on quasi-steady regimes, since most current SCM convection schemes effectively make some form of quasi-steady assumption. Clearly the representation of convective activity on timescales shorter than the life cycle of a convective cloud system may require some model of that life cycle that goes beyond the scope of most current parametrizations. Time-development under the diurnal cycle is specifically addressed in other parts of the EUROCS project in a manner complementary to the present study.

In quasi-steady problems one needs to consider carefully the specification of forcing. For if we prescribe 'forcing' tendencies (viewed as radiative, large-scale or artificial), and require convection to balance those in quasi-equilibrium, then we have effectively prescribed the convective tendencies themselves. Such specifications can give many theoretical insights, but experience with GCMs is that changes to the convection parametrization can lead to changes in circulations and large-scale forcing. Hence, in the present intercomparison, we need a testbed that allows some simple feedback between convection and larger scales.

We chose here to specify a simple feedback model by representing external forcing via the nudging of the mean profiles to prescribed target profiles of the form

$$(\partial\phi/\partial t)_{\mathrm{nudging}} = \{\phi_{\mathrm{t}}(z) - \overline{\phi}(z)\}/t_{\mathrm{n}}, \tag{1}$$

where ϕ is a generic model variable, $\overline{\phi}$ the horizontal mean (as normally computed in an SCM or CRM), $\phi_{\mathrm{t}}(z)$ the target profile and t_{n} a nudging timescale. Note that this prescribed feedback does not damp the fluctuating variables, i.e. no direct contribution

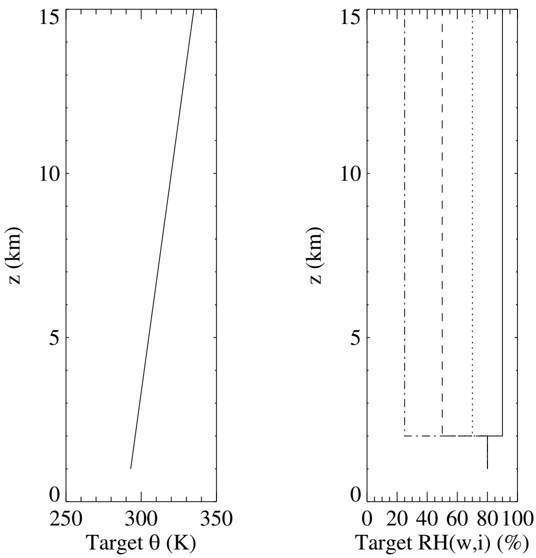

Figure 1. Sketch of the specified target profiles for the cloud-resolving and single-column model intercomparison. No values are shown below 1 km as there is no nudging there in the standard case. From 1 km, θ increases with height at a constant rate 3 K km^{-1}. Above 2 km the target humidities $\mathrm{RH_t}$ differ, as indicated by the following key: $\mathrm{RH_t} = 90\%$ (solid line), 70% (dotted line), 50% (dashed line) or 25% (dot-dashed line).

to the variance of ϕ at any given height. This nudging of means was applied here to potential temperature θ, specific humidity q_v and horizontal wind $\mathbf{u}$ with a nudging timescale of one hour.

The method of nudging mean profiles has been used, for example, by Randall and Cripe (1999), and can also be justified as a simpler less radical approximation to the testbed of Sobel and Bretherton (2000), where the virtual-temperature profile is assumed to be fixed by strong large-scale feedback. Note that (despite some 'large-scale' motivation) the present set-up can be viewed simply as a testbed for comparison without needing to correspond precisely to 'large-scale forcing' in any atmospheric column.

Since we are considering quasi-steady situations, the forcing profiles are in balance with the apparent heat and moisture sources, and therefore can be inferred directly when we diagnose these terms later.

(*a*) *Case specification*

The humidity intercomparison case for CRMs and SCMs was specified using target profiles for potential temperature and humidity, as sketched in Fig. 1. The specification is based on three layers, respectively a 'boundary layer' below 1 km, a 'transition layer' 1–2 km and 'free troposphere' above 2 km.

The target profile for potential temperature $\overline{\theta}(z)$ was specified to increase linearly with height at a rate 3 K km^{-1} from a value of 293 K at 1 km. This implies a dry static stability close to the 'standard' tropospheric value 10^{-4} s^{-2}, with moderate instability to adiabatic moist ascent. Radiative effects are excluded, but may be considered as implicit in the target temperature profile.

The target relative humidity RH(w,i) was specified as 80% in the transition layer, but constant values of 25%, 50%, 70% or 90% in the free troposphere. Here RH(w,i) denotes the higher value of the relative humidities with respect to water or ice. This ensures that the target profiles are subsaturated with respect to both phases at all heights.

TABLE 1. SUMMARY OF PARTICIPATING SINGLE-COLUMN MODELS

Source	Version	Convection scheme	Participants
Met Office	UM4.5	Gregory–Rowntree (3C)	Derbyshire
LMD	N1A	Emanuel, adapted	Grandpeix
ECMWF	IFS	Tiedtke	Bechtold
ECMWF	IFS-MNH	Bechtold et al.	Bechtold, Soares
Météo-France	ARPEGE-NWP	Bougeault–Geleyn	Piriou
Météo-France	ARPEGE-CLIMAT	v1: Bougeault	Beau
		v2: Gueremy-Grenier	Beau

These profiles can be regarded as idealizations of the observed profiles discussed by Johnson (1997).

A target wind-profile was also set at $U_t(z) = (0.5 \text{ m s}^{-1}) \ln(1 + z/z_0)$ where $z_0 =$ 0.1 m. This moderate-strength and monotonic profile would be expected to promote surface evaporation, but not to give strong convective organization. As the SCMs differ significantly in their treatment of the free-convective surface layer, which is not the main focus of this study, the inclusion of a mean wind helps us avoid that regime.

The 'boundary layer' (below 1 km) was excluded from the nudging, as we wished to allow SCM boundary-layer schemes to develop their own preferred structure, so that we could effectively test the convective representation. For different reasons, Sobel and Bretherton (2000) also used a separate treatment for the boundary layer. In the absence of nudging, the target profile is, therefore, undefined in that layer. As shown later, a sensitivity test was conducted to the inclusion of boundary-layer nudging.

The surface potential temperature, θ, was set at 294 K, thus ensuring moderate instability across the boundary layer. Surface pressure was specified as 1000 hPa. Surface humidity was treated as saturated (i.e. effectively as a sea surface). For simplicity a roughness length $z_0 = 0.1$ m was applied to the scalar variables as well as momentum. Each model used its own standard surface-transfer algorithm based on Monin–Obukhov theory (the Met Office CRM surface algorithm is as described by Tompkins (2001b)).

(*b*) *Description of participating models*

This intercomparison includes two CRMs and six SCMs, as listed in Table 1, with both CRMs run in three-dimensional (3D) mode.

The Met Office CRM is an anelastic model developed as an extension of a boundary-layer large-eddy simulation (LES) code. The bulk cloud microphysics are based on cloud water, rain, ice, snow and graupel categories with double-moment options (Swann 1998). Here, we used double moment for ice only. The model has been validated extensively for boundary-layer, shallow-convection and deep-convection applications (Petch and Gray (2001), and references), including observational comparisons of deep convection with data from the UK radar, the ARM–SGP* facility and TOGA-COARE.

The CNRM–GAME† CRM is the model of Redelsperger *et al.* (2002). This model is also anelastic but has many differences from the Met Office CRM. The CNRM–GAME model uses a different (turbulent kinetic energy (TKE) based) turbulence scheme, as well as partial condensation and differences in ice microphysics. It has been developed and tested against tropical convection, squall lines, frontal systems and shallow convection. Redelsperger *et al.* (2002) have given further details and references.

* Atmospheric Radiation Measurement–South Great Plains.

† Centre National de Recherches Météorologiques–Groupe d'etude de l'Atmosphere Météorologique.

In this study we adopted a 500 m horizontal resolution as standard for the CRMs. One of them was also run at a 250 m resolution. In the CRM literature these models are often run at horizontal resolutions of 1–2 km (see Petch and Gray (2001) for discussion and references). The horizontal domain specification was periodic with a length of 48 km as standard (but sensitivity to doubling this length was tested, as described below). As is normal with this type of model, the vertical resolution was non-uniform with height. The Met Office CRM was run with 48 levels, giving an average vertical resolution around 300 m, comparable with the horizontal resolution, but around 100 m vertical resolution in the boundary layer (see also the appendix for a sensitivity test to higher resolution). The CNRM vertical resolution was slightly coarser, with 38 levels.

The SCMs are single-column versions of either global or mesoscale models. The Met Office SCM is the single column version of the Met Office global model version 4.5. Its convection scheme (3C) is based on that of Gregory and Rowntree (1990), with extensions for downdraughts, convective momentum transport and a CAPE closure.

The SCM of the European Centre for Medium-Range Weather Forecasts (ECMWF) Integrated Forecast System (IFS) was run with two alternative convection schemes. Owing to the practicalities of running within the forecast system, radiative effects were left on in this SCM. However, these are not expected to have major effects in this case (we verified that the radiative heating was small compared with the convective heating).

First of all, the IFS was run with its standard physics, including 'Tiedtke convection' based on that of Gregory *et al.* (2000) and Tiedtke (1989). The convective available potential energy (CAPE) closure was assigned a one-hour adjustment time. In this configuration, turbulent entrainment was assigned a value 10^{-4} m^{-1} for deep convection and 3×10^{-4} m^{-1} for shallow clouds, but increased by a factor varying from 4 at cloud base to 1 at 150 hPa above cloud base. An additional representation of organized convection is applied to deep clouds, with detrainment a function of updraught velocity. The IFS was also run alternatively with 'Meso-NH convection' following the scheme of Bechtold *et al.* (2001).

The ARPEGE* global model exists in two main versions with substantially different physics, and here we treat the numerical weather prediction (NWP) and climate versions (or the SCMs drawn from each) as separate models.

The ARPEGE-NWP SCM includes convective representation based on the mass-flux scheme of Bougeault (1985), with subsequent modifications following Geleyn *et al.* (1982) and Ducrocq and Bougeault (1995) for downdraughts. It also includes some recent changes to entrainment representation, including an element of adaptation tending to maintain the ratio of dilute to adiabatic parcel buoyancy excess (cf. Swann 2001).

ARPEGE-CLIMAT SCM was first run with its version-3 standard physics, including a mass-flux convection scheme based on that of Bougeault (1985) and a moist diffusion scheme (Ricard and Royer 1993). The convection scheme was used with a three-hour adjustment time CAPE closure. Additionally, ARPEGE-CLIMAT was run with revised convection and diffusion schemes (v2 due to Gueremy and Grenier, personal communication). This revision concerns mass-flux, entrainment and triggering condition for the convection scheme, and mixing length and entrainment at the top of the boundary layer for the diffusion scheme. The new convection scheme is based on a convective vertical velocity that affects the entrainment and detrainment rates within a buoyancy-sorting framework (whereas the original version computed entrainment with an analytical function depending on the convection depth).

* Action de Recherche Petite Echelle et Grand Echelle.

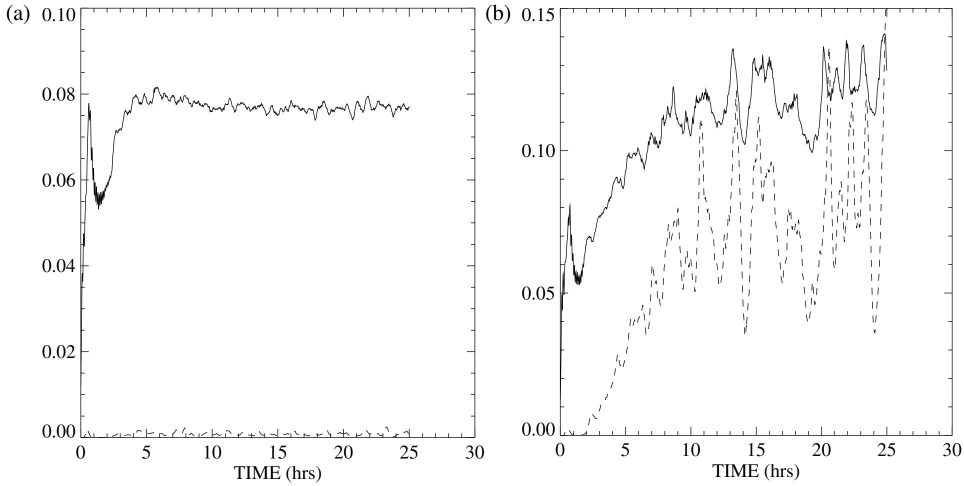

Figure 2. Typical time-development of convective activity. Illustrative plot from Met Office cloud-resolving model at 250 m resolution with $\mathrm{RH_t}$ = (a) 0.25 or (b) 0.7 (mass flux averaged over whole domain (solid line), and surface precipitation rate (cm hr^{-1}) (dashed line)).

The LMD† SCM is the single-column version of the LMDZ GCM (Doutriaux-Boucher and Quaas 2004). It contains an adapted version of the Emanuel (1991) convection scheme. The N1A version modified the original Emanuel scheme (1) by removing some explicit grid dependencies in the lifting condensation level, triggering and closure and (2) in the use of ice thermodynamics, strengthening the unsaturated downdraughts. A second version, N1B, included, additionally, a complete reformulation of the mixing probability distribution, as described by Grandpeix *et al.* (2004).

3. CRM AND SCM RESULTS

(*a*) *CRM results*

Figure 2 shows time-series of basic measures of convective activity from the Met Office model at high resolution (250 m). The diagnostics were, respectively, surface precipitation and a measure of cloudy mass flux over the whole domain, chosen arbitrarily as a simple average over all model points purely as a gross diagnostic for time-variation in convection. These time-series typically become ‘statistically steady’ by 12 hours. The surface precipitation time-series shows greater random time variation than the mass-flux time-series, presumably reflecting the episodic nature of precipitation events even within the lifetime of an individual convective cloud. To minimize statistical variation, the Met Office CRM results were averaged over the final 12 hours (i.e. from approximately 12–24 hours into the run). Because the CRMs resolve the fluctuating convective fields, they are expected to show short-period fluctuations in the mass flux and other statistics, even if the mean profiles are essentially steady. An SCM, however, might be expected to run steadily under steady forcing (if its parametrizations are supposed themselves to represent ensemble averages).

Figure 3 illustrates the horizontal distributions of hydrometeors, again within the Met Office CRM at high resolution. Figure 3(a) shows cloud liquid water q_l at 2 km, with patterns of open-cell organization resembling those in satellite imagery as described

† Laboratoire de Météorologie Dynamique.

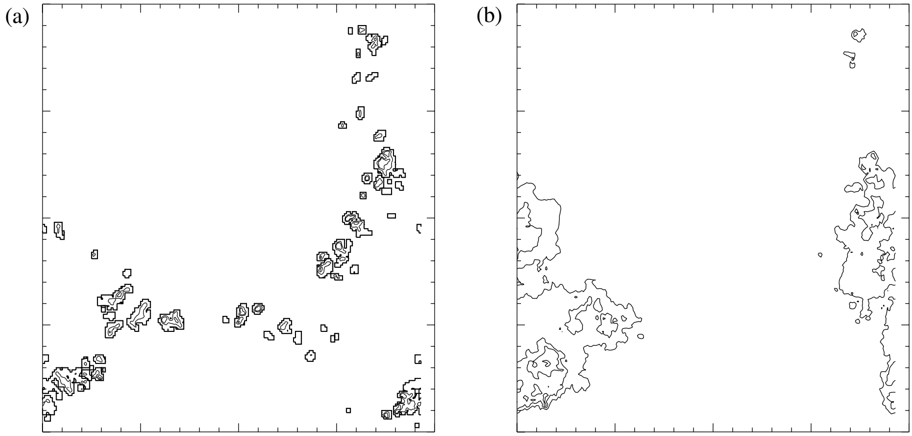

Figure 3. Simultaneous snapshots of hydrometeor distribution in horizontal slices for illustration of typical cloud-resolving model (CRM) fields (here using the Met Office CRM at 250 m resolution and with $\mathrm{RH_t} = 0.7$, from the final period of the run). (a) Cloud liquid water q_l at $z = 2$ km, with the zero-contour shown bold (maximum value 2.2 g kg^{-1}), and (b) Cloud ice at $z = 8$ km (maximum 1.9 g kg^{-1}).

by Bader *et al.* (1995), whilst Fig. 3(b) shows larger cloud-ice shields at 8 km. Other plots (not shown) indicated that the liquid-water cores were numerically reasonably well resolved.

Figure 4 shows quasi-steady profiles of cloudy updraught mass flux (using the widest definition based on all cloudy updraught points) from the Met Office CRM at 500 m and 250 m horizontal resolution. A clear systematic impact of the mid-tropospheric humidity is evident in both versions, with the moist case $\mathrm{RH_t} = 0.9$ giving strong convection with an elevated peak, whereas the driest case $\mathrm{RH_t} = 0.25$ gives shallow convection with mass flux decreasing monotonically with height above cloud base.

The agreement between the 500 m and 250 m resolutions is also quantitatively good for the more moist cases, which have deep convection. In LES we might expect the resolution-convergence of a 3D simulation of convection of depth H to be governed by the resolution normalized by H. By this measure, a simulation of 10 km deep convection at 250 m resolution is similar to a simulation of 1 km deep convection at 25 m resolution and (insofar as our problem resembles classical LES problems) should be well resolved. Indeed the subgrid components of the mean fluxes were also found to be small in the present problem. Whilst some caution is appropriate, owing to the physical complexity of deep convective clouds, the numerical robustness found here is very encouraging.

However, the driest case ($\mathrm{RH_t} = 0.25$) has shallow convection and is found to be more sensitive to resolution (as is consistent with our scaling argument). At the higher resolution the shallow convection has a shape typically found in shallow-cumulus LES intercomparisons against observations (Brown *et al.* 2002). The type of resolution sensitivity found here for shallow convection is broadly consistent with some previous LES tests (A. R. Brown, personal communication—see also Petch and Gray (2001) and references).

Figure 4(c) shows corresponding results with a 500 m horizontal resolution when the nudging region is extended to the whole domain, including the boundary layer. For this profile, the target θ was set at 293 K and the target q_v at 8 g kg^{-1} in the boundary layer. The deep-convection cases show little sensitivity to boundary-layer nudging,

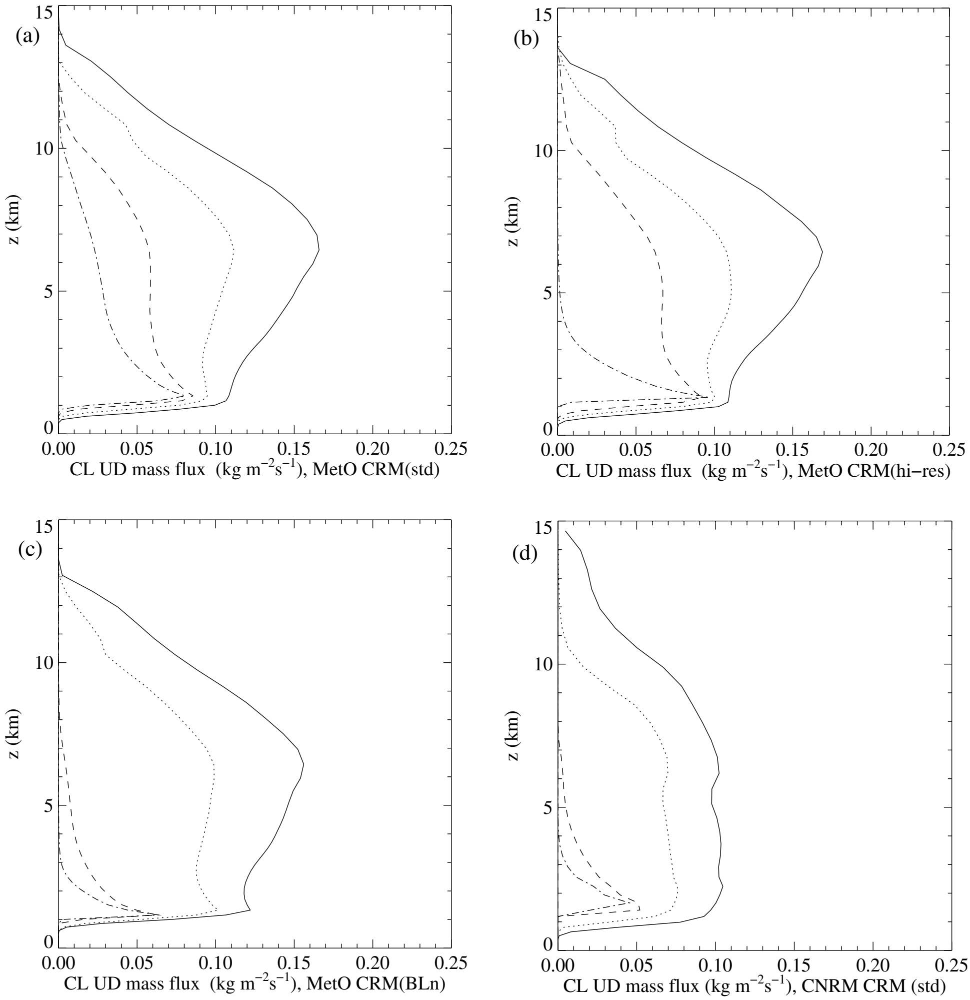

Figure 4. Cloudy updraught mass flux profiles for the four RH_t values in the cloud-resolving models (CRMs): the Met Office CRM at (a) 500 m, (b) 250 m, (c) 500 m with boundary-layer nudging (see text), and (d) the CNRM–GAME CRM at the standard 500 m horizontal resolution (line definitions as in Fig. 1). Note that all four plots are on the same scales.

although there is significant impact on the drier, shallow cases, with a slight widening in the gap between shallow and deep convection. Some sensitivity to this significant change in the specified set-up is to be expected, but evidently boundary-layer nudging does not diminish the humidity sensitivity.

Corresponding updraught mass-flux results for the CNRM–GAME CRM at 500 m resolution are shown in Fig. 4(d). The overall agreement with the Met Office CRM is generally good, especially as the set-up was chosen to maximize the possible differences between models. The basic transition from shallow to deep convection as a function of RH_t is well reproduced. The shallow convection in the CNRM–GAME CRM is slightly shallower, extending to about 4 km as against 5 km in the Met Office CRM, although these differences are smaller than the resolution sensitivity shown in the previous figure. The CNRM–GAME model gives a clearer transition from shallow to deep convection

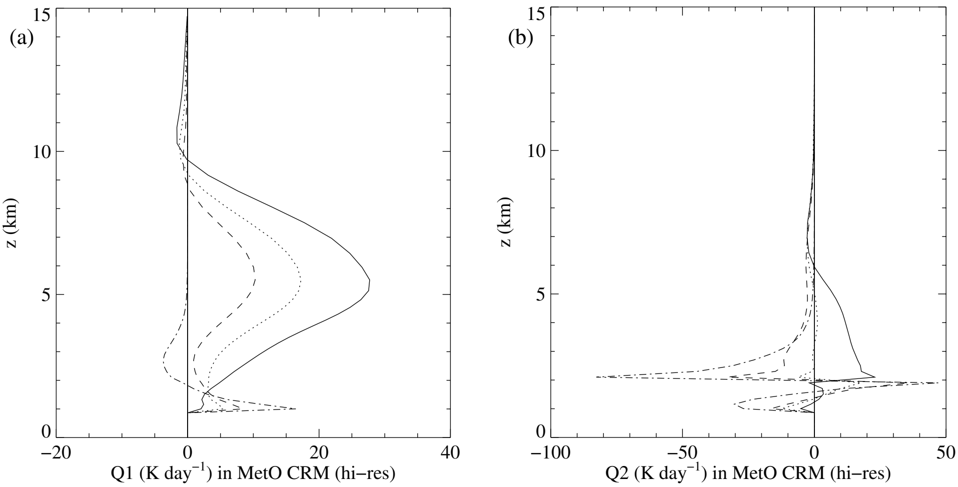

Figure 5. The apparent heating and drying rates (a) Q1 and (b) Q2 in the Met Office cloud-resolving model at 250 m resolution (line definitions as in Fig. 1).

than the Met Office model, and a plateau rather than an elevated peak for mass flux in the case $\mathrm{RH_t} = 90\%$. As is seen later, these differences are relatively subtle compared with the range of differences arising in the SCMs (see also the Q1 discussion below).

The insensitivity to horizontal resolution in the Met Office CRM suggests that the subgrid turbulence scheme is not critical (at least for the deep convection cases). It seems likely that most of the differences between the two CRMs arise from either (1) the partial condensation scheme in the CNRM–GAME model as against simple condensation in the Met Office model or (2) microphysical differences, including the treatment of cold cloud. Given the independent formulations of these two CRMs, these differences provide one measure of remaining uncertainty in modelling this problem.

The sensitivity of cloud-base mass flux in the CRMs to $\mathrm{RH_t}$ is limited. The Met Office CRM gives only 20–25% more mass flux when $\mathrm{RH_t} = 0.9$ than when $\mathrm{RH_t} = 0.25$, although there is vigorous precipitation in the former but almost none in the latter. This finding is consistent with the hypothesis that the boundary layer can exert significant controls even over vigorous deep convection.

Figure 5 shows the apparent heating and drying rates $Q1 = (\partial T/\partial t)_{\mathrm{convection}}$ and $Q2 = -(L/c_p)(\partial q/\partial t)_{\mathrm{convection}}$, in the conventional notation, as evaluated with the Met Office CRM at the higher horizontal resolution. Figure 6 shows corresponding results with the CNRM–GAME model. It can be seen that the Q1 results are closely linked to the mass flux, and that the two CRMs agree well in Q1 except for the case $\mathrm{RH_t} = 0.5$ where, as previously noted, the mass fluxes differ. In fact, for the case $\mathrm{RH_t} = 0.9$ the agreement between CRMs in Q1 is noticeably better than in updraught mass flux. Note that, unlike Q1, a 'mass flux' is ultimately a diagnostic quantity with inevitable arbitrariness in its definition (especially in a very moist atmosphere), and can include some 'inactive' or reversible motion in which a parcel ascends and then descends before completing the mixing assumed in mass-flux theory.

Q2 may be considered a less robust quantity (e.g. sensitive to local detrainment) but the overall agreement between CRMs is still reasonably good. The sharp variations around 2 km (especially in the driest case, with its shallow convection) are consequences

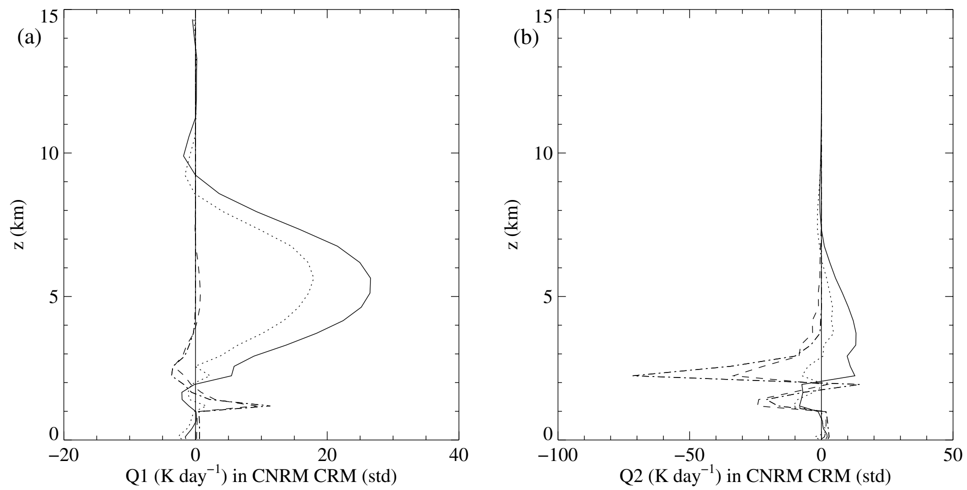

Figure 6. The apparent heating and drying rates (a) Q1 and (b) Q2 in the CNRM–GAME cloud-resolving model at the standard 500 m horizontal resolution (line definitions as in Fig. 1).

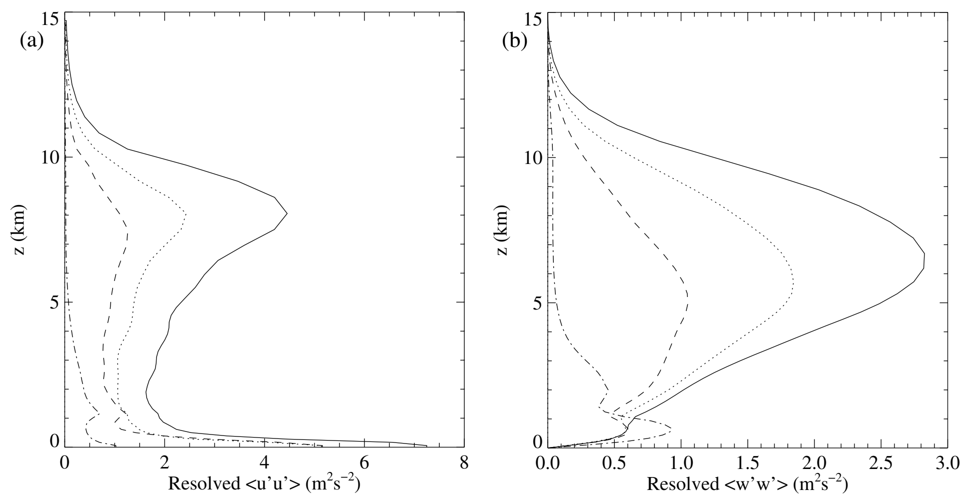

Figure 7. Profiles of resolved velocity variances for (a) $\overline{u'^2}$ (stream wise) and (b) $\overline{w'^2}$ (vertical) in the Met Office cloud-resolving model at 250 m horizontal resolution for the four values of RH_t (line definitions as in Fig 1).

of the mass flux penetrating the level of a step change in the target profile, and represent the erosion of that humidity step.

Figure 7 shows profiles of resolved velocity variances from the Met Office CRM at high resolution, and Fig. 8 indicates the corresponding flux profiles. These profiles confirm that the differences between runs at different values of RH_t involve substantial dynamical differences. The driest case $RH_t = 0.25$ shows velocity-variance profiles dominated by peaks in the boundary layer, not very different from boundary-layer simulations (e.g. Mason 1989). In contrast, the more moist runs show variance and flux peaks at much higher levels. Qualitatively, the shapes of the deep-convecting velocity-variance profiles resemble boundary-layer profiles, only with the height scale increased

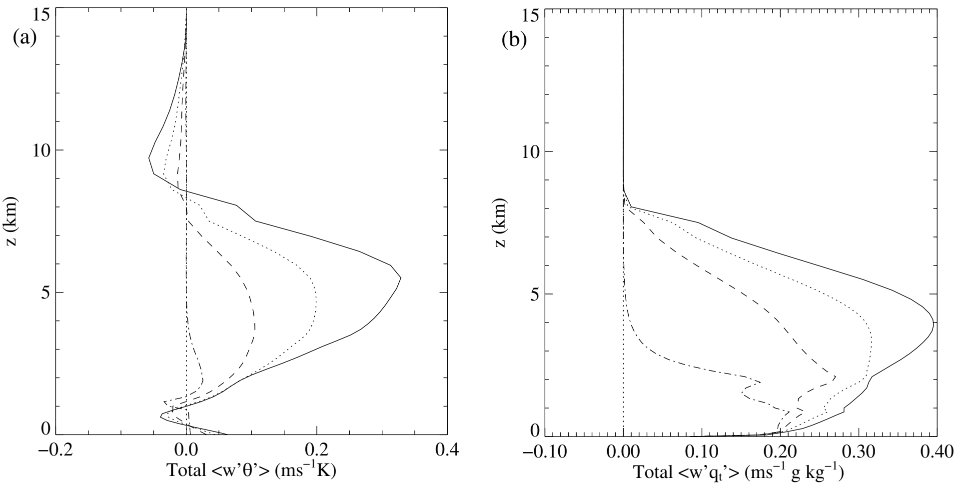

Figure 8. Profiles of total kinematic fluxes for (a) $\overline{w'\theta'}$ and (b) $\overline{w'q_t'}$ in the Met Office cloud-resolving model at 250 m horizontal resolution for the four values of RH_t (line definitions as in Fig. 1). The variable q_t denotes total water vapour plus liquid cloud droplets.

by a factor approaching 10. For the deep-convecting cases these statistics broadly resemble the findings of Khairoutdinov and Randall (2002), though since we are not solving the same problem we do not expect exact correspondence.

Figure 8 also shows how the surface fluxes change in association with the convective activity. The surface sensible-heat flux, in particular, adjusts to 'recharge' the boundary layer from the cooling due to convection.

(*b*) *SCM results in comparison with CRM results*

Figure 9 shows parallel results for updraught mass-flux profiles from the CRMs and some of the SCMs, all plotted on the same scales. The CRM results are discussed above but replotted to aid comparison. Figure 9(c) shows results with IFS-MNH, with mass fluxes comparable to the CRM profiles for $RH_t = 0.7$, but little adaptation in response to more moist or drier conditions. In contrast (Fig. 9(d)) the ARPEGE-NWP SCM, here with a three-hour CAPE adjustment timescale, adapts substantially to humidity and gives shallow convection in the driest case. The IFS-Tiedtke SCM (Fig. 9(e)) again gives profiles comparable to the CRMs for $RH_t = 0.7$, but has limited adaptation to humidity.

The Met Office SCM (Fig. 9(f)) shows some adaptation to RH_t, with deeper convection in the more moist cases, but does not closely match the CRM results. The SCM shows a strong tendency for the mass flux to peak sharply in the upper troposphere in all the subcases. The discrepancy is especially clear in the dry case, where the CRMs show a shallow-cumulus regime with mass flux decreasing monotonically above cloud base.

The LMD version N1A scheme (Fig. 10(a)) shows in our test problem a strong elevated peak at heights ~7–8 km for all the values of RH_t, with significant mass flux penetrating well above 10 km. Of all the schemes tested, this seems the most nearly adiabatic in its behaviour. The LMD scheme was then modified with changes to the mixing fraction. This modified version is called N1B and is shown in Fig. 10(b), for $F_0 = 0.65$, where the tunable parameter F_0 is approximately the modal value of the

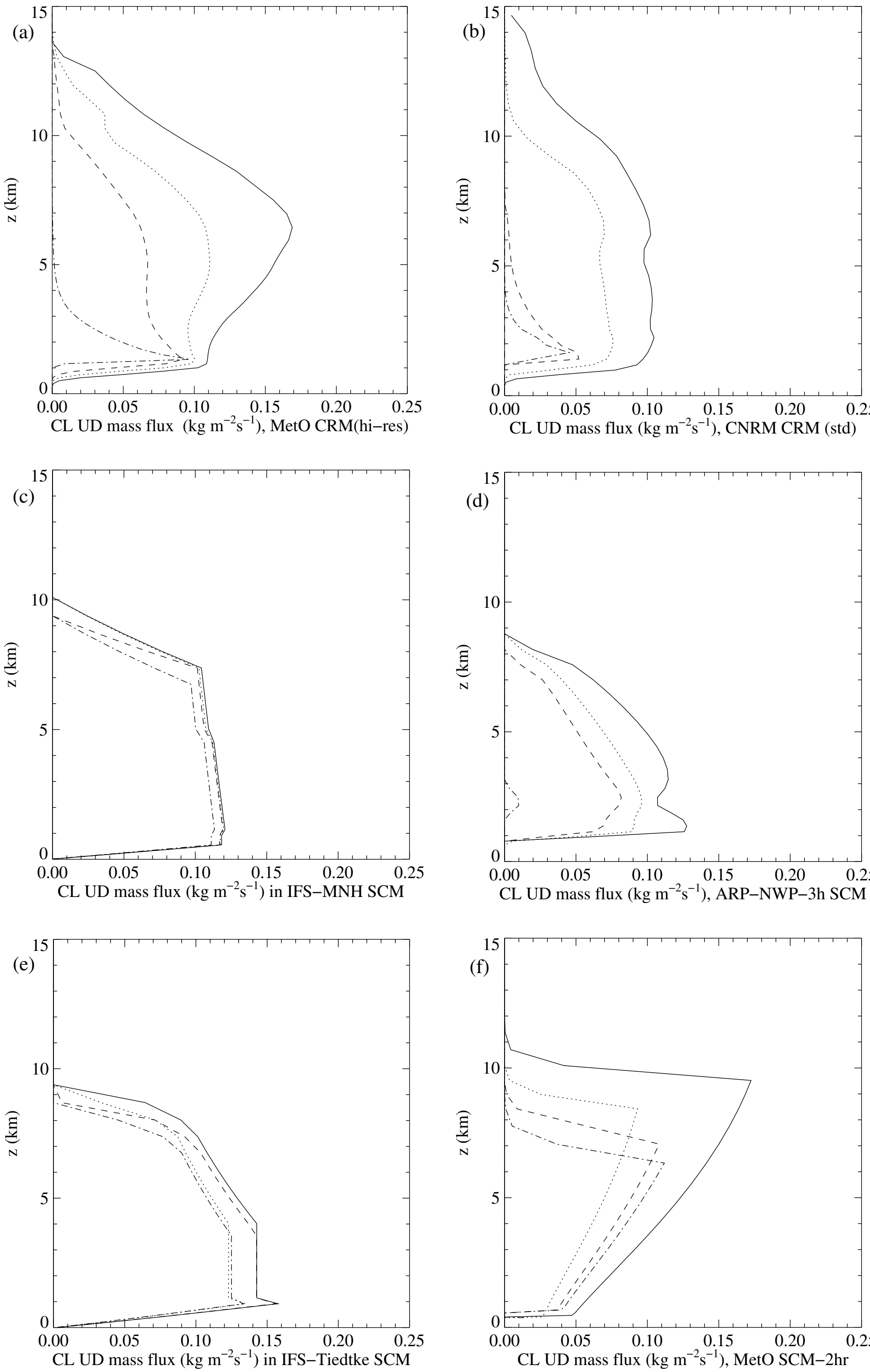

Figure 9. Mass-flux comparisons of six models in the humidity case, all plotted on the same scales: the cloud-resolving runs of (a) the Met Office and (b) CNRM, and the single-column runs of (c) IFS-MNH, (d) ARP-NWP, (e) IFS-Tiedke, and (f) the Met Office (line definitions as in Fig. 1).

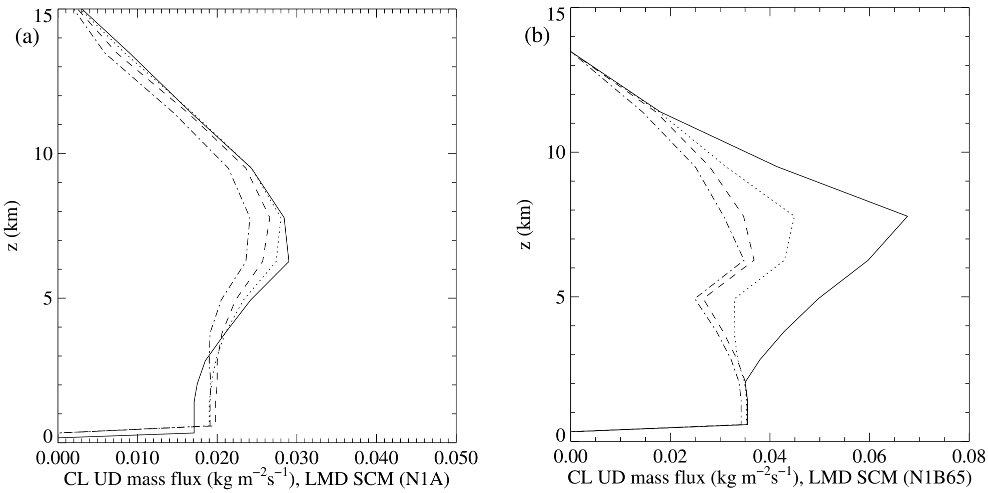

Figure 10. Updraught mass fluxes in the LMD single-column model versions (a) N1A and (b) N1B (the latter using $F_0 = 0.65$) (line definitions as in Fig. 1). See text for further details.

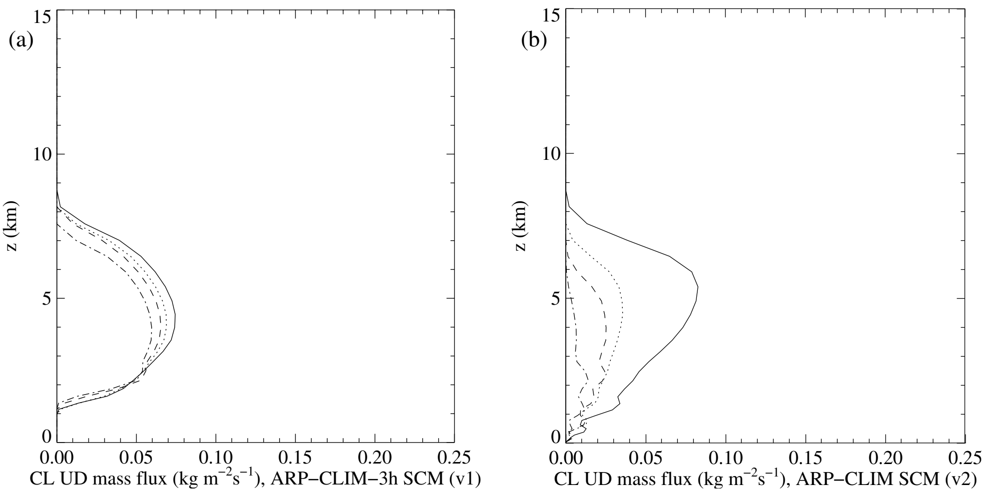

Figure 11. Updraught mass-flux profiles from the ARPEGE-CLIMATE SCM: (a) an old version (three-hour timescale), and (b) a new version with Gueremy–Grenier physics (line definitions as in Fig. 1).

mixing-fraction distribution. Grandpeix *et al.* (2004) have described this in detail and show the sensitivity of mass-flux profile shapes to F_0.

The LMD results (both N1A and N1B) give generally smaller mass fluxes than the other schemes or the CRMs, but this is probably not a fundamental issue as these mass fluxes could be easily increased by retuning the closure.

As noted above, the ARPEGE-CLIMAT SCM was extensively revised during this intercomparison in its convection and other physics. Figure 11 shows that the Gueremy–Grenier revision (v2) led to mass-flux profiles that were much closer to the CRM behaviour, with greater adaptivity to the humidity.

Potentially the most precise comparisons between CRMs and SCMs are of the apparent temperature source Q1 and apparent drying Q2 (Figs. 12 and 14). However,

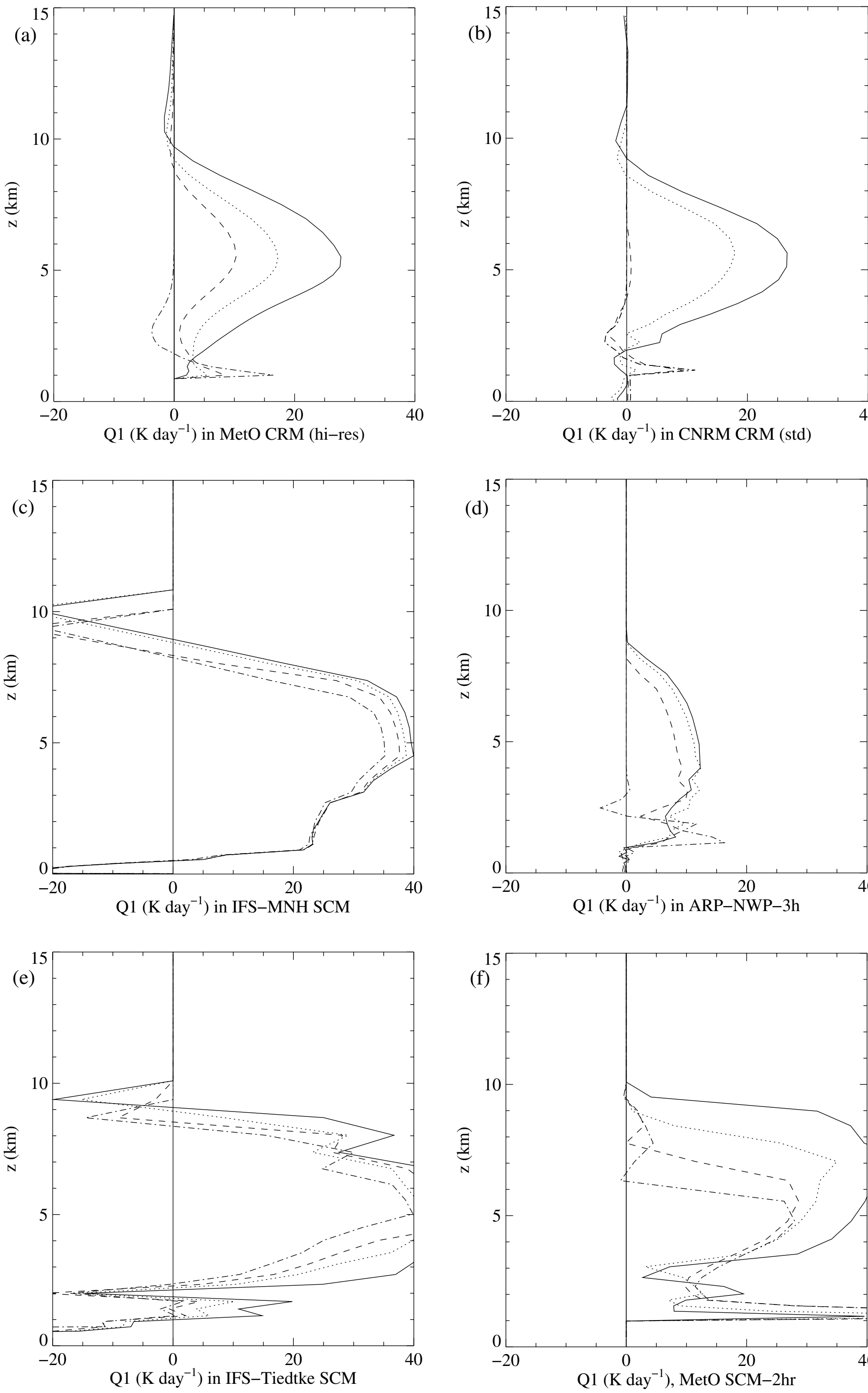

Figure 12. Comparisons in apparent convective heating Q1 (K day^{-1}) of six models in the humidity case, all plotted on the same scales (layout of panels as in Fig. 9 and line definitions as in Fig. 1).

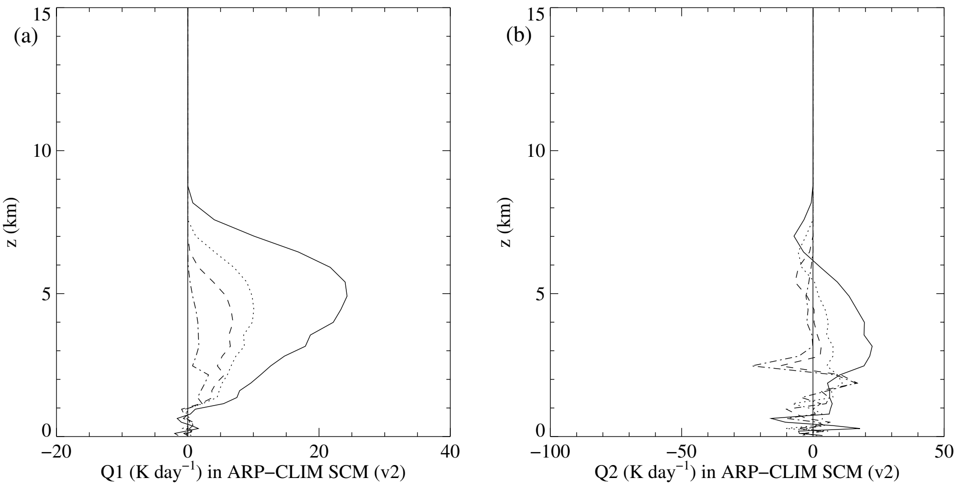

Figure 13. Profiles of the apparent heating and drying rates (a) Q1 and (b) Q2 from the ARPEGE-CLIMATE SCM with v2 physics (Gueremy–Grenier) (line definitions as in Fig. 1). See text for further details.

since the convective heating and drying involve vertical derivatives of sensible- and latent-heat fluxes, or within a mass-flux approximation certain detrainment terms, the Q1 and Q2 profiles in an SCM have some sensitivity to the vertical derivative of mass flux. Within a mass-flux framework (e.g. Gregory and Rowntree 1990) Q1 and Q2 can be written as 'clear-air subsidence plus detrainment'. For Q1 the updraught virtual-potential-temperature excess θ_v' is usually small over most of the profile, compared with the clear air $\partial\theta_v/\partial z$. Hence Q1 is roughly a measure of clear-air subsidence which, by continuity, corresponds to the net in-cloud mass flux. A loose correspondence can indeed be seen in the SCM Q1s and the corresponding updraught mass fluxes, with some notable exceptions.

The IFS-MNH SCM shows for Q1, as for mass flux, limited sensitivity to RH_t. A notable feature is the cooling by detrainment at the top of the convecting layer, around 9–10 km. The ARP-NWP SCM again shows significantly different profile shapes, and greater adaptivity to RH_t. This SCM exhibits a 'shallow convection' regime in the driest case, which again matches the CRMs quite well. It does not show any negative Q1s at the top of deep convection, but captures the negative Q1 at the top of the shallow-convection layer in the driest case. The IFS–Tiedtke SCM shows some similarities to IFS-MNH, including the upper detrainment-cooling layer. However, it is somewhat more RH_t adaptive, and differs significantly in its low-level structure. The Met Office SCM shows some problems in handling the layer 1–2 km that have been found in other investigations to reflect problems in diagnosing the depth of the boundary layer in this version. In the mid troposphere the profile shapes of Q1 very loosely capture those of the CRMs, except for the driest case where the shallow-convection regime is not well captured.

The ARPEGE-CLIMAT v2 SCM shows an even greater adaptivity of Q1 to RH_t (Fig. 13), consistent with its adaptivity of the mass flux.

The apparent drying rate, Q2, is evidently one of the more difficult quantities for the SCMs to capture in detail, not least because of the mass transport across strong vertical gradients in specific humidity. However, it can be seen that where the SCMs show good

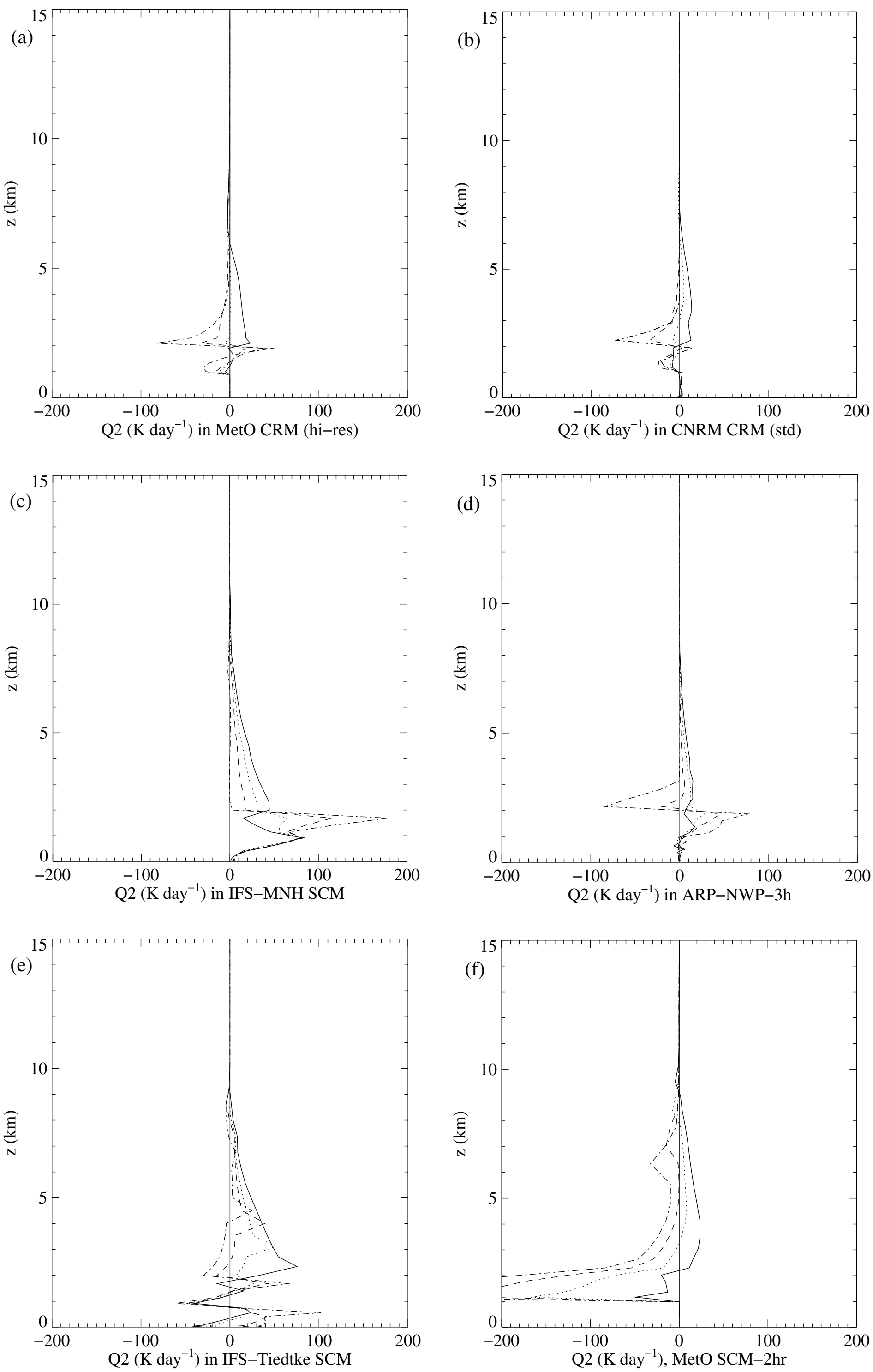

Figure 14. Comparisons of the apparent convective drying rates Q2 (K day^{-1}) of six models in the humidity case, all plotted on the same scales (layout of panels as in Fig. 9 and line definitions as in Fig. 1). The off-scale values are discussed in the text.

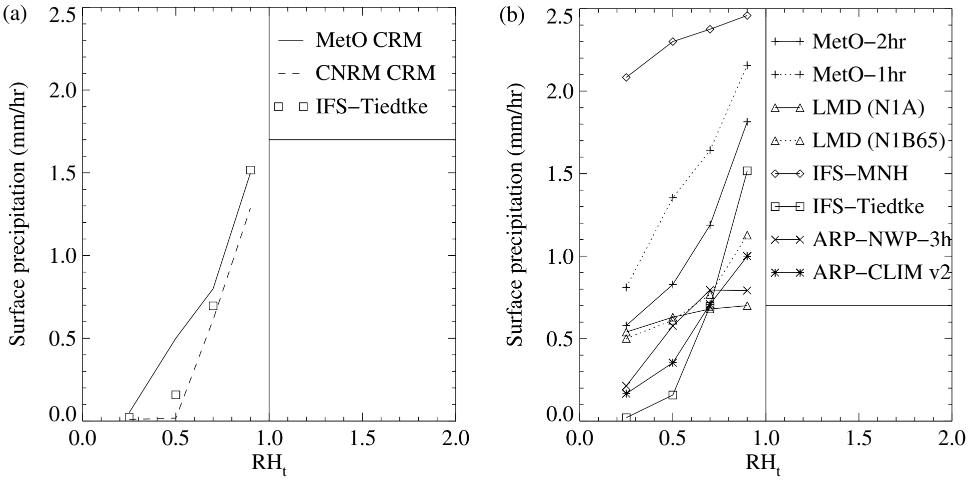

Figure 15. Surface precipitation rates in quasi-steady period as function of RH$_t$: (a) the cloud-resolving models (with the IFS-Tiedtke single-column model (SCM) also shown) (b) all the SCMs, including a sensitivity test of the closure timescale in the Met Office SCM and of the different versions of the LMD scheme.

agreement with the CRMs in mass flux they, typically, also show at least a fair agreement in Q2.

The IFS-MNH SCM (Fig. 14(c)) shows a strong drying tendency at almost all levels, even for the drier cases. This model seems to have a particularly high precipitation efficiency (as is evident in later discussion when we consider surface precipitation). In contrast, the ARP-NWP SCM shows reasonable overall agreement with the CRMs, except for the layer 1–2 km which it predominantly dries, but the CRMs moisten. The ARP-CLIMAT v2 SCM agrees overall perhaps even better, and is the closest of the SCMs to matching the CRMs in the layer from 1–2 km. The IFS-Tiedtke SCM shows again predominantly drying behaviour, with some indications of numerical issues in the lower layers.

The Met Office SCM captures the drying in the moist cases relatively well but stands out in its strong tendency to moisten the layer from 1–2 km (in contrast to the ARP-NWP SCM, for instance). This moistening gives off-scale values as large as -350 K day^{-1} for Q2 in that layer. It has been found that some versions of the corresponding GCM can give excessive moistening of a kind broadly consistent with this finding.

(*c*) *Surface precipitation*

Figure 15 compares the average surface precipitation rates in the quasi-steady period obtained from the participating models. The CRMs show a strong dependence of surface precipitation on the RH$_t$ parameter. For RH$_t = 0.25$, the surface precipitation is only a trace value, whereas for RH$_t = 0.9$ the value is around 1.3–1.6 mm h^{-1}. The comparison tells broadly the same story as the mass flux, with overall good quantitative consistency between the models, except for the transition case RH$_t = 0.5$, which the CNRM model treats as shallow, but the Met Office CRM treats as intermediate.

The SCMs all show some increase in precipitation with RH$_t$, and comparable magnitudes to the CRMs, but with significant variations in detail. Most of the SCMs give significant surface precipitation, even in the driest case, unlike both CRMs.

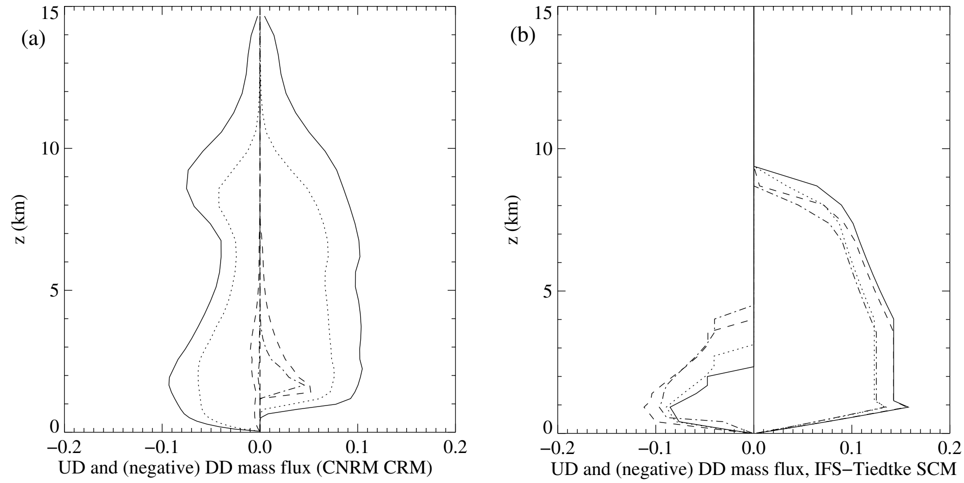

Figure 16. Downdraught and updraught mass fluxes (kg $s^{-1}m^{-2}$) in (a) the CNRM-GAME cloud-resolving model and (b) the IFS-Tiedtke single-column model. For each case, the downdraughts are plotted with the same line style as the updraughts, but with a negative sign (line definitions as in Fig. 1).

The IFS-Tiedtke SCM lies within the envelope of the CRMs for all the RH_t values tested, including the driest case. However, detailed investigation showed that, in this SCM, precipitation was produced even in the driest case (substantial mass flux extending as high as 8 km, as shown above) but evaporated in the downdraught scheme. This finding illustrates the need to look at a number of diagnostics, not just surface precipitation. Indeed, there might be some scope for tuning surface precipitation via closure timescales, if that were the only concern.

4. Role of downdraughts and boundary-layer interactions

So far we have focused on updraughts as a primary measure of convective activity, related at least roughly to Q1 (cf. Figs. 9 and 12). However downdraughts can play a significant role, particularly in the interaction with the boundary layer.

Both downdraughts and updraughts may be viewed as part of a complex set of feedbacks between (1) free-tropospheric mean profiles (2) fluctuating activity in the boundary layer and free troposphere (including convective updraughts and downdraughts) (3) boundary-layer mean profiles and (4) surface fluxes.

Figure 16 plots cloudy downdraughts and updraughts in one of the CRMs (CNRM) and one of the SCMs (IFS-Tiedtke). This SCM matches the CRM downdraughts reasonably well in the lower troposphere, for the intermediate case $RH_t = 0.7$. The diagnosed CRM downdraughts in the upper troposphere may not, in any case, be the most relevant choice for parametrization. Comparison with Q1 above suggests significant cancellation between CRM updraught and downdraught impacts, consistent with recirculation within cloudy air rather than irreversible impacts on the environment. However, the SCM downdraughts, like the updraughts, show much less adaptation to RH_t than the CRMs.

Part of the theoretical significance of downdraughts is as a mechanism for modifying the boundary-layer moist static energy, h, as discussed by Raymond (2000) and Tompkins (2001a,b). A positive perturbation to mid-tropospheric q (and thus h), if

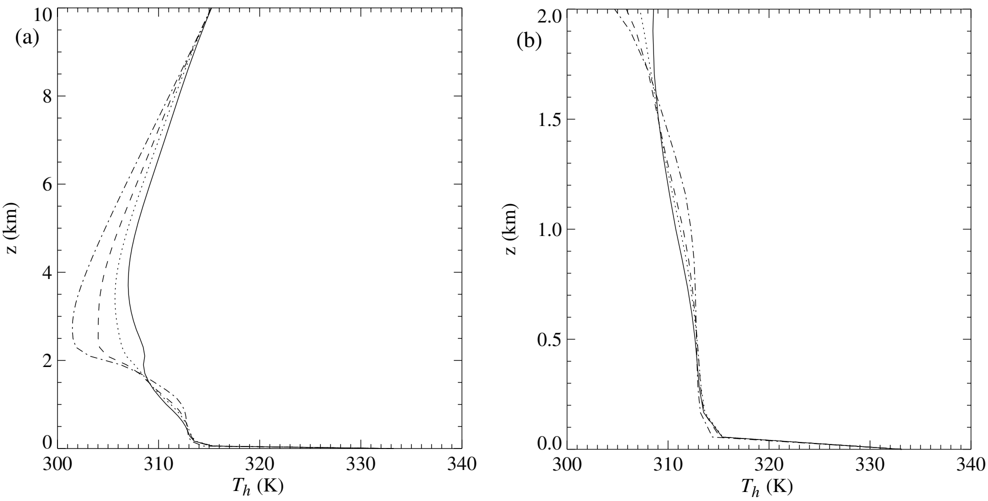

Figure 17. Moist-static-energy temperature (T_h) profiles from the four RH_t runs with the Met Office cloud-resolving model at 250 m horizontal resolution, shown (a) up to 10 km and (b) up to 2 km. Note the crossover around 1.6 km (line definitions as in Fig. 1).

transported downwards, could influence positively the boundary layer h, and hence the potential for convection.

To examine the possible role of such downward controls in the present case, consider the profiles of moist-static-energy temperature, T_h, (Fig. 17). These show that T_h in the upper boundary layer changes in the *opposite* sense to the mid-tropospheric changes due to variation in RH_t. These suggest that, at least in these simulations, downdraught feedbacks through the boundary-layer (BL) thermodynamic budgets are a secondary effect in opposition to the primary mechanism of updraught mixing.

The interpretation of the mechanism

$$\text{free-troposphere mean profiles} \rightarrow \text{BL mean profiles} \rightarrow \text{fluctuating activity}$$

as secondary is also consistent with the nudging results of Fig. 4(c), in which nudging the boundary layer (thus limiting the downdraught impact) was found to *widen* the gap between the driest case and the others.

There is a small variation in T_h in the surface layer (at around 100 m) in the same sense as in the mid troposphere, but this seems attributable to enhanced surface exchange as convection becomes more active (cf. near-surface horizontal gusts in Fig. 7). The results are consistent with downdraughts playing a significant role in re-triggering convective activity.

In summary, our CRM results appear to imply a primary direct humidity impact

$$\text{free-troposphere mean profiles} \rightarrow \text{fluctuating activity,}$$

with compensating negative feedbacks through

$$\text{free troposphere mean profiles} \rightarrow \text{BL mean profiles} \rightarrow \text{activity.}$$

This negative feedback is itself limited by the negative feedback

$$\text{BL mean profiles} \leftrightarrow \text{surface fluxes,}$$

which recharges the boundary layer.

5. Conclusions

The significance of free-tropospheric humidity for convection is increasingly recognized (Raymond and Zeng 2000; Raymond 2000; Tompkins 2001a; Ridout 2002). These impacts are significant for large-scale modelling through the coupling to vertical motion (e.g. Grabowski 2003), and to quasi-horizontal dry intrusions (Redelsperger *et al.* 2002).

We designed an idealized quasi-steady case to show quantitatively the impact of mid-tropospheric humidity on convection and to intercompare these impacts in cloud-resolving and single-column models. The results show significant humidity impacts, which are qualitatively consistent with the predictions of entraining-plume theory, but also show limitations of current mass-flux schemes. The most striking humidity impact is that a dry mid-tropospheric profile (say 25% relative humidity) can suppress deep convection in favour of a shallow convection regime.

In formulating this case, given our underlying aim of helping GCM parametrization, we noted that the dynamical interaction of a finite region of convection with the large-scale atmosphere constrains the mean profiles more strongly in a GCM than in process studies without such feedback. Sobel and Bretherton (2000) have developed a testbed for SCMs which assumes that the temperature profile is fully under large-scale control, from which the vertical velocity, and hence humidity forcing, may be diagnosed. Here, we chose a set-up that is broadly similar in spirit, but slightly less radical, by relaxing the mean profiles to prescribed target values on a one-hour timescale. This nudging is applied only above the boundary layer, in order to test convection schemes rather than boundary-layer schemes. We also specified a monotonic target wind profile, which promotes mechanically driven turbulent exchange from the sea surface, but is not expected to give strong mesoscale organization of the convection. Provided that we intercompare consistently between the CRMs and SCMs, this testbed need not correspond exactly to any specific observed case.

The two CRMs used here were formulated independently and tested in a range of previous case studies. In particular, the formulations for cloud, microphysics and turbulence are completely independent and have not been tuned to agree in this case. The level of agreement between the CRMs can, therefore, be viewed as a fair indication of underlying confidence. In fact, the quantitative agreement between the CRMs is generally good. The updraught mass-flux profiles are mostly very similar, with one major exception, namely that the case $\mathrm{RH_t} = 0.5$ case is more similar to the case $\mathrm{RH_t} = 0.25$ in the CNRM-GAME model, whereas in the Met Office model it appears transitional between shallow and deep regimes. The updraught mass fluxes at $\mathrm{RH_t} = 0.9$ also show some differences at upper levels. The agreement in the Q1 and Q2 profiles, except in this one transitional case, is also good, and at $\mathrm{RH_t} = 0.9$ the agreement is considerably better in Q1 than in the mass flux (perhaps reflecting the arbitrariness in the definition of the latter). These diagnostics give a complementary picture of the major impacts of humidity.

Sensitivity tests in the Met Office CRM show an encouraging robustness in the main results. Halving the horizontal grid length from 500 m to 250 m has no significant impact on the more moist more deeply convecting cases. The profile of shallow convection in the driest case is slightly affected by refinement of resolution, which brings the Met Office CRM results closer to those of the CNRM-GAME model. Insensitivity to resolution in such models is normally a sign also of insensitivity to turbulence representation. Other tests showed that doubling the horizontal domain sizes, or changing the detailed method of nudging, also made little difference.

We focused here on the quasi-steady period, since time-development is studied systematically in other parts of the EUROCS project. However we note that the approach to quasi-steady convection in the present CRM runs takes appreciably longer than the profile-nudging timescale. This finding is consistent with the view that the delay in developing fluctuating activity in cloud systems (as opposed to mean-profile adjustment alone) can be significant in problems such as the convective diurnal cycle.

The SCMs show some humidity sensitivity in precipitation at least, but also a strong tendency for most convection schemes to give their own ‘preferred’ shapes of mass-flux profiles. For instance, the Met Office SCM, based on the Gregory–Rowntree scheme with prescribed entrainment rates, shows strong elevated peaks in the updraught mass-flux profile, and fails to adapt its mass-flux profile shapes to different humidity environments in the manner of the CRMs. Nevertheless, it shows a strong dependence of surface precipitation on humidity which is not too far from the CRMs. Some SCMs, e.g. ARPEGE-NWP, give substantial humidity adaptation in the mass fluxes. In the ARPEGE-CLIMAT SCM, the v2 revision gave a much improved match to the CRM results. Other schemes, such as the IFS-Tiedtke scheme, show more limited humidity adaptivity in the mass-flux profile, although this does not necessarily prevent substantial humidity sensitivity in the surface precipitation. A fundamental problem seems to be the need to move decisively beyond the simple entraining-plume model and represent a strong element of variability within the cloud ensemble (whether through adaptive plume parameters, buoyancy-sorting, multi-plume schemes or other approaches). Sensitivity tests (in particular with the LMD scheme) suggest that, in some existing convection schemes, the variability component can be usefully enhanced.

For schemes with tunable adjustment timescales the values matching the CRM results most closely are typically 1–3 hours, consistent with previous GCM experience.

Our CRMs show significant downdraughts (penetrating into the boundary layer), which the IFS-Tiedtke SCM matches reasonably well in the more moist cases. However, the moist static energy of the boundary layer varies in the opposite sense to that of the free troposphere as we vary RH_t, in contrast to the simplest notions that moist-static-energy transport by downdraughts regulates moist convection through the boundary-layer moist-static-energy budget. This is consistent with the finding (in CRM tests) that extension of nudging to the boundary layer acted to increase the humidity sensitivity.

We do not exclude a significant role for downdraughts in triggering secondary convection, and in quantitatively modifying the humidity sensitivity. Nevertheless, it seems clear that there are primary humidity impacts on the updraughts that most current SCMs do not handle well, owing to the limited ability of most convection schemes to adapt entrainment and detrainment to environmental conditions that are favourable or unfavourable for convection. Results from LMD, ARPEGE-NWP and ARPEGE-CLIMAT all suggest that greater adaptivity in updraught mixing models can give more credible humidity sensitivities.

Several tests related to this case have been carried out in GCMs. Whilst this work is ongoing, and its documentation outside the scope of this paper, we briefly note the typical findings. In the LMD model, humidity sensitivity was found to affect convection in GCMs around continental margins. The modifications tested in the SCM gave significant improvements to the GCM representation of the West African monsoon (Grandpeix *et al.* 2004). In the Met Office model, introducing a humidity sensitivity in the closure timescale helped prevent unrealistic convective disturbances. It was also found helpful to use information about the sign of w as a secondary criterion, in addition to inversion-based diagnosis, to help distinguish shallow or deep convection; this can be viewed as a proxy for humidity. The version of the Bougeault–Geleyn scheme, which performed well in the present tests, is now operational in ARPEGE-NWP. The revised

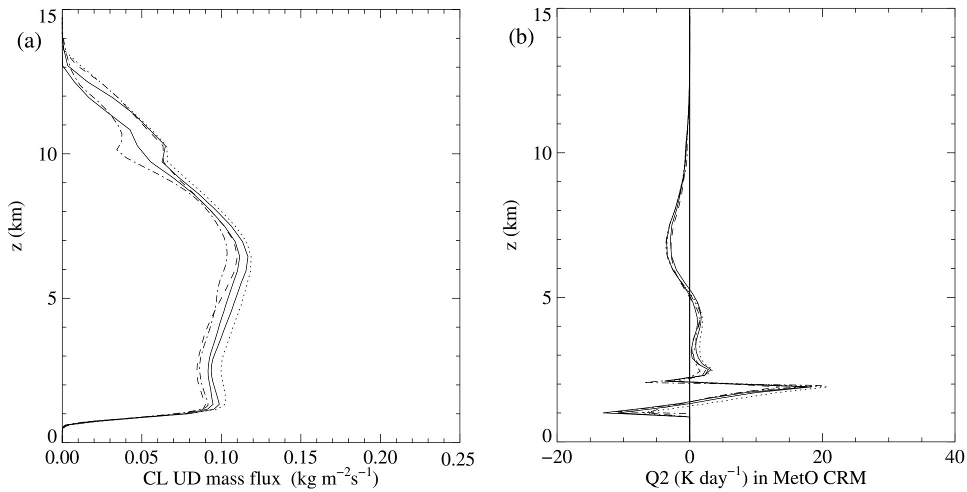

Figure A.1. Sensitivity tests with the Met Office CRM at 500 m horizontal resolution with $RH_t = 0.7$ for (a) cloudy updraught mass flux, and (b) Q2: standard run (solid line); large domain (dotted line); run with nudging in clear air only (dashed line); doubled number of levels (dot-dashed line). On each panel the standard run is plotted twice, from averages at 50 000–70 000 s and 70 000–90 000 s, respectively, to show the degree of quasi-steadiness.

IFS-Tiedtke scheme, developed using this case and other tests, is now operational at ECMWF. These GCM tests add to the findings of Grabowski (2003) that convective sensitivity to humidity can play an important role in large-scale dynamics.

Despite the evidence of numerical robustness in the CRMs, the present results are not claimed to be the last word on this problem. For instance, it would be inappropriate to tune Q2 in the SCMs to the CRM values beyond the level of consistency of the latter. However, we are encouraged that this intercomparison has already shed light on the various convection schemes involved, especially in their mass-flux structure. Future extensions to this methodology are of course possible, as are further uses of this case to test SCM changes.

Acknowledgements

This work was made possible by a European Union grant EVK2 CT1999 0005. We thank F. Guichard and J. Petch for discussions and assistance with diagnostics, P. Marquet and J. F. Gueremy for comments on ARPEGE-CLIMAT, B. Mapes and M. Miller for encouragement, and the EUROCS community for lively and productive workshops. A. Brown, W. Grabowski, R. Kershaw, P. Siebesma, A. Tompkins and the reviewers gave incisive comments which helped improve the paper.

Appendix

CRM sensitivity tests

Further tests were conducted into the sensitivity of CRM results to numerical parameters (Fig. A.1), relative to the control run with 48 km × 48 km horizontal domain, 500 m horizontal resolution, 48 levels and nudging active on all points above 1 km. A ‘large-domain’ test was conducted with 96 km × 96 km horizontal domain but still with 500 m horizontal resolution. A ‘clear-air-only’ nudging run, limiting nudging to non-cloudy points, and a 'high-vertical-resolution' test using 96 levels were also conducted.

Results for all these tests (shown for updraught mass flux and Q2) show encouraging robustness to all these numerical parameters and choices. Whilst the differences are not entirely negligible, they are smaller than the physical impacts shown above of RH_t values or different SCMs and physics schemes. The unsteadiness is also fairly small. We therefore consider the CRM results a suitable basis for the present intercomparison.

At the beginning of EUROCS we also conducted a pilot simulation using simplified cloud physics, and with the nudging timescale set to zero (with target profiles enforced as a hard constraint). The results were qualitatively very similar to the standard intercomparison run, with similar profile shapes and transitions with changing humidity.

REFERENCES

Arakawa, A. and Schubert, W. H. 1974 Interaction of a cumulus cloud ensemble with the large-scale environment. *J. Atmos. Sci.*, **31,** 674–701

Bader, M., Forbes, G. S., Grant, G. R., Lilley, R. B. E. and Waters, A. J. 1995 *Images in weather forecasting: A practical guide for interpreting satellite and radar imagery*. Cambridge University Press, UK

Bechtold, P., Bazile, E., Guichard, F., Mascart, P. and Richard, E. 2001 A mass flux convection scheme for regional and global models: *Q. J. R. Meteorol. Soc.*, **127,** 869–886

Blyth, A. M., Cooper, W. A. and Jensen, J. B. 1988 A study of the source of entrained air in Montana cumuli. *J. Atmos. Sci.*, **45,** 3944–3964

Bougeault, P. 1985 A simple parameterization of the large-scale effects of cumulus convection. *Mon. Weather Rev.*, **113,** 2108—2121

Brown, A. R., Cederwall, R. T., Chlond, A., Duynkerke, P. G., Golaz, J.-C., Khairoutdinov, M., Lewellen, D. C., Lock, A. P., MacVean, M. K., Moeng, C.-H., Neggers, R. A. J., Siebesma, A. P. and Stevens, B. 2002 Large-eddy simulation of the diurnal cycle of shallow cumulus convection over land. *Q. J. R. Meteorol. Soc.*, **128,** 1075–1093

Donner, L. J. 1993 A cumulus parameterization including mass fluxes, vertical momentum dynamics, and mesoscale effects. *J. Atmos. Sci.*, **50,** 889–906

Dourtriaux-Boucher, M. and Quaas, J. 2004 Evaluation of cloud thermodynamic phase parametrization in the LMDZ GCM by using POLDER satellite data. *Geophys. Res. Lett.*, **31,** 6126–6130

Ducrocq, V. and Bougeault, P. 1995 Simulations of an observed squall line with a meso-beta scale hydrostatic model, *Weather and Forecasting*, **10,** 380–399

Emanuel, K. A. 1991 A scheme for representing cumulus convection in large-scale models. *J. Atmos. Sci.*, **48,** 2313–2335

Geleyn, J.-F., Girard, C. and Louis, J.-F. 1982 A simple parameterization of moist convection for large-scale atmospheric models, *Beitr. Phys. Atmos.*, **55,** 325–334

Grabowski, W. 2003 MJO-like coherent structures: Sensitivity simulations using the cloud-resolving convection parameterization (CRCP). *J. Atmos. Sci.*, **60,** 847–864

Grandpeix, J.-Y., Phillips, V. and Tailleux, R. 2004 Improved mixing representation in Emanuel's convection scheme. *Q. J. R. Meteorol. Soc.*, **130,** 3207–3222

Grant, A. L. M. and Brown, A. R. 1999 A similarity hypothesis for shallow-cumulus transports. *Q. J. R. Meteorol. Soc.*, **125,** 1913–1936

Gregory, D. and Rowntree, P. R. 1990 A mass-flux convection scheme with representation of cloud ensemble characteristics and stability-dependent closure. *Mon. Weather Rev.*, **118,** 1483–1506

Gregory, D., Morcrette, J. J., Jakob, C., Beljaars, A. C. M. and Stockdale, T. 2000 Revision of convection, radiation and cloud schemes in the ECMWF integrated forecast system, *Q. J. R. Meteorol. Soc.*, **126,** 1685–1710

Johnson, R. H. 1997 'Recent observations of deep convection: TOGA–COARE'. Pp. 1–24 in *New insights and approaches to convective parametrization*. ECMWF, Reading, UK

Kain, J. S. and Fritsch, J. M. 1990 A one-dimensional entraining/detraining plume model and its application in convection parametrization. *J. Atmos. Sci.*, **47,** 2784–2802

Khairoutdinov, M. F. and Randall, D. A. 2002 Similarity of deep continental cumulus convection as revealed by a three-dimensional cloud-resolving model. *J. Atmos. Sci.*, **59,** 2550–2566

Mason, P. J. 1989 Large-eddy simulation of the convective boundary layer. *J. Atmos. Sci.*, **46,** 1492–1516

Petch, J. C. and Gray, M. 2001 Sensitivity studies using a cloud-resolving model simulation of the tropical west Pacific. *Q. J. R. Meteorol. Soc.*, **127,** 2287–2306

Randall, D. A. and Cripe, D. G. 1999 Alternative methods for specification of observed forcing in single-column models and cloud systems models. *J. Geophys. Res.*, **104,** 24527–24545

Raymond, D. J. 2000 Thermodynamic control of tropical rainfall. *Q. J. R. Meteorol. Soc.*, **126,** 889–898

Raymond, D. J. and Zeng, X. 2000 Instability and large-scale circulations in a two-column model of the tropical troposphere. *Q. J. R. Meteorol. Soc.*, **126,** 3117–3135

Redelsperger, J. L., Parsons, D. B. and Guichard, F. 2002 Recovery processes and factors limiting cloud-top height following the arrival of a dry intrusion observed during TOGA–COARE. *J. Atmos. Sci.*, **59,** 2438–2457

Ricard, J. L. and Royer, J. F. 1993 A statistical cloud scheme for use in an AGCM. *Ann. Geophys.*, **11,** 1095–1115

Ridout, J. A. 2002 Sensitivity of tropical Pacific convection to dry layers at mid to upper levels: Simulation and parameterization tests. *J. Atmos. Sci.*, **59,** 3362–3381

Riehl, H. 1954 *Tropical meteorology*. McGraw-Hill, New York

Sobel, A. H. and Bretherton, C. S. 2000 Modeling tropical precipitation in a single column. *J. Climate*, **13,** 4378–4392

Swann, H. A. 1998 Sensitivity to the representation of precipitating ice in CRM simulations of deep convection. *Atmos. Res.*, **48,** 415–435

2001 Evaluation of the mass flux approach to parametrizing deep convection. *Q. J. R. Meteorol. Soc.*, **127,** 1239–1260

Tiedtke, M. 1989 A comprehensive mass-flux scheme for cumulus parameterization in large-scale models. *Mon. Weather Rev.*, **117,** 1779–1800

Tompkins, A. M. 2001a Organization of tropical convection in low vertical wind shears: The role of water vapor. *J. Atmos. Sci.*, **58,** 529–545

2001b Organization of tropical convection in low vertical wind shears: The role of cold pools. *J. Atmos. Sci.*, **58,** 1650–1672

Xu, K.-M., Cederwall, R. T., Donner, L. J., Grabowski, W. W., Guichard, F., Johnson, D. E., Khairoutdinov, M., Krueger, S. K., Petch, J. C., Randall, D. A., Seman, C. J., Tao, W. K., Wang, D., Xie, S. C., Yio, J. J. and Zhang, M. H. 2002 An intercomparison of horizontal resolution on the ARM Summer 1997 IOP data. *Q. J. R. Meteorol. Soc.*, **128,** 1095–1135

Zhang, C., Mapes, B. E. and Soden, B. J. 2003 Bimodality in tropical water vapour. *Q. J. R. Meteorol. Soc.*, **129,** 2847–2866